RAA 2014 Vol. **14** No. **5**, 589–600 doi: 10.1088/1674–4527/14/5/008
http://www.raa-journal.org *http://www.iop.org/journals/raa*

Research in Astronomy and Astrophysics

Electromagnetic effects on the orbital motion of a charged spacecraft

Yehia Ahmed Abdel-Aziz[1,2] and Khalil Ibrahim Khalil[1]

[1] National Research Institute of Astronomy and Geophysics (NRIAG), Helwan, Cairo 11721, Egypt; *yehia@nriag.sci.eg*

[2] Department of Mathematics, Hail University, Hail 2440, Kingdom of Saudi Arabia

Received 2013 May 6; accepted 2013 November 5

Abstract This paper deals with the effects of electromagnetic forces on the orbital motion of a spacecraft. The electrostatic charge which a spacecraft generates on its surface in the Earth's magnetic field will be subject to a perturbative Lorentz force. A model incorporating all Lorentz forces as a function of orbital elements has been developed on the basis of magnetic and electric fields. This Lorentz force can be used to modify or perturb the spacecraft's orbits. Lagrange's planetary equations in the Gauss variational form are derived using the Lorentz force as a perturbation to a Keplerian orbit. Our approach incorporates orbital inclination and the true anomaly. The numerical results of Lagrange's planetary equations for some operational satellites show that the perturbation in the orbital elements of the spacecraft is a second order perturbation for a certain value of charge. The effect of the Lorentz force due to its magnetic component is three times that of the Lorentz force due to its electric component. In addition, the numerical results confirm that the strong effects are due to the Lorentz force in a polar orbit, which is consistent with realistic physical phenomena that occur in polar orbits. The results confirm that the magnitude of the Lorentz force depends on the amount of charge. This means that we can use artificial charging to create a force to control the attitude and orbital motion of a spacecraft.

Key words: space vehicles — atmospheric effects — celestial mechanics — kinematics and dynamics

1 INTRODUCTION

The orbital and attitude motion of an electrostatically charged spacecraft in orbit around the Earth is subject to the Lorentz force in the Earth's magnetic field. Juhász & Horányi (1997) studied objects in a degrading orbit around the Earth as well as solid rocket motors generating micron- and submicron-sized space debris. They showed that the motion of these particles is dictated by gravity, solar radiation pressure and electromagnetic forces. As these grains collect electrostatic charges, their dynamics start to be influenced by electric and magnetic fields in the Earth's magnetosphere, and that magnetospheric effects tend to reduce the lifetime of these grains either by forcing them onto elliptical orbits that collide with the Earth or by swiftly ejecting them into interplanetary space.

Several attempts have been made to assess the effects of the Lorentz force to show that, in principle, it is negligible compared to some other important effects (e.g. Sehnal 1969). However, the necessary high precision of orbital determination in some proposed space experiments (Ciufolini et al. 1993) requires full knowledge of the electrodynamic effects connected with the Lorentz force, which we shall try to study in detail. Vokrouhlicky (1989) determined the orbital effects of the Lorentz force on the motion of an electrically charged artificial satellite moving in the Earth's magnetic field. In this case, the influence of the geomagnetic field predominantly manifests itself by the Lorentz force.

The Lorentz spacecraft is a nascent concept that artificially generates a net electrostatic charge on a spacecraft to provide propulsive accelerations for orbit control. Therefore, the Lorentz force can be used to change and control the orbit of the spacecraft without consuming propellant (Peck 2005). Abdel-Aziz (2007) studied the effects of an approximate Lorentz force on the orbital motion in Low Earth Orbit (LEO). Streetman & Peck (2007) investigated the Lorentz-augmented orbits and used them to accomplish a variety of complex orbital behaviors for new types of geosynchronous orbits. Pollock et al. (2011) studied the relative motion of a charged spacecraft subject to perturbations from the Lorentz force due to interactions with the planetary magnetosphere.

In the present paper, the total Lorentz force is developed in two cases: (1) the Lorentz force experienced by a geomagnetic field and (2) the Lorentz force experienced by an electric dipole moment in the presence of an electric field. The total Lorentz force which is generated due to the electrostatic charges in the Earth's magnetosphere is derived as a function of orbital elements. Gauss variational equations are used to derive the time rate of change in the orbital elements of the spacecraft. The numerical results show that the effect of the Lorentz force due to its magnetic component is three times greater than the effect of the Lorentz force due to its electrical component. The results also show that the perturbation in the orbital elements of the spacecraft is a second order perturbation due to the Lorentz force. In addition, the numerical results confirm that the strong effects are due to the Lorentz force in a polar orbit, which is consistent with realistic physical phenomena that occur in a polar orbit. The results confirm that the magnitude of the Lorentz force depends on the charge to mass ratio. This means we can use artificial charging to create a desired force which is needed to control the attitude and orbital motion of a spacecraft.

In Section 2 we develop the total Lorentz force as a function of orbital elements. Section 3 describes the rate of change in the orbital elements due to Lorentz force using Lagrange planetary equations in Gauss form. Section 4 introduces numerical results, which show the effects of the Lorentz force on the orbital elements for two different satellites.

2 THE TOTAL LORENTZ FORCE

We use spherical coordinates to describe the magnetic and gravitational fields, and the spacecraft trajectory, as shown in Figure 1. The x, y and z axes form a set of inertial Cartesian coordinates. The Earth is assumed to rotate about the z-axis. The magnetic dipole is not tilted and is therefore axisymmetric. The spherical coordinates consist of radius r, colatitude angle ϕ and azimuth from the x direction θ (see Fig. 1).

The magnetic field is expressed as

$$\boldsymbol{B} = \frac{B_0}{r^3}\left[2\cos\phi\,\hat{\boldsymbol{r}} + \sin\phi\hat{\boldsymbol{\phi}} + 0\hat{\boldsymbol{\theta}}\right], \tag{1}$$

where B_0 is the magnetic dipole moment in Wb m.

The acceleration in inertial coordinates is given by

$$\boldsymbol{a} = \frac{\boldsymbol{F}}{m} = -\frac{\mu}{r^3}\boldsymbol{r} + \frac{q}{m}(\boldsymbol{E} + \boldsymbol{V}_{\rm rel} \times \boldsymbol{B}), \tag{2}$$

where $\frac{q}{m}$ is the charge to mass ratio of the spacecraft and $\boldsymbol{V}_{\rm rel}$ is the velocity of the spacecraft relative to the magnetic field of the Earth. The total Lorentz force (per unit mass) can be written as

$$\boldsymbol{F}_{\rm L} = \frac{q}{m}\left[\boldsymbol{E} + \boldsymbol{V}_{\rm rel} \times \boldsymbol{B}\right] = \frac{q}{m}\boldsymbol{E} + \frac{q}{m}(\boldsymbol{V}_{\rm rel} \times \boldsymbol{B}) = \boldsymbol{F}_{\rm elec} + \boldsymbol{F}_{\rm mag}, \tag{3}$$

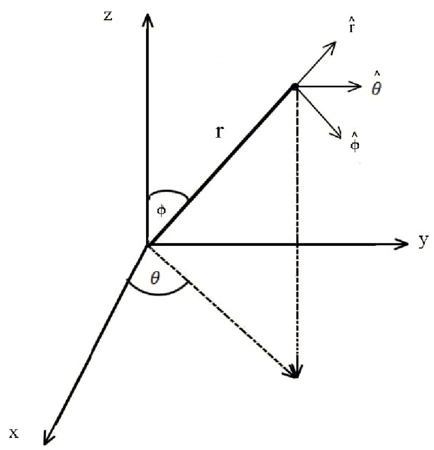

Fig. 1 Spherical coordinates used in the derivation of the equations of motion.

where $\boldsymbol{F}_{\mathrm{mag}}$ is the Lorentz force due to the geomagnetic field and $\boldsymbol{F}_{\mathrm{elec}}$ is the Lorentz force experienced by an electric dipole moment in the presence of an electric field,

$$\boldsymbol{F}_{\mathrm{elec}} = \frac{q}{m}\boldsymbol{E}\,. \tag{4}$$

Now we start with $\boldsymbol{F}_{\mathrm{mag}}$, and by using Streetman & Peck (2007), we can write

$$\boldsymbol{F}_{\mathrm{mag}} = \frac{q}{m}(\boldsymbol{V}_{\mathrm{rel}} \times \boldsymbol{B})\,, \tag{5}$$

$$\boldsymbol{V}_{\mathrm{rel}} = \boldsymbol{V} - \boldsymbol{\omega}_{\mathrm{e}} \times \boldsymbol{r}\,, \tag{6}$$

where $\boldsymbol{V}$ is the inertial velocity of the spacecraft and $\boldsymbol{\omega}_{\mathrm{e}}$ is the angular velocity vector of the Earth. According to Streetman & Peck (2007), we use

$$\boldsymbol{V} = \dot{r}\hat{\boldsymbol{r}} + r\dot{\phi}\,\hat{\boldsymbol{\phi}} + r\dot{\theta}\sin\phi\hat{\boldsymbol{\theta}} \tag{7}$$

and

$$\boldsymbol{r} = r\,\hat{\boldsymbol{r}}\,, \tag{8}$$

$$\boldsymbol{\omega}_{\mathrm{e}} = \omega_{\mathrm{e}}\,\hat{\boldsymbol{z}}\,, \tag{9}$$

$$\hat{\boldsymbol{z}} = \cos\phi\hat{\boldsymbol{r}} + \sin\phi\hat{\boldsymbol{\phi}}\,. \tag{10}$$

Therefore, the acceleration in inertial coordinates is given by

$$\boldsymbol{F}_{\mathrm{mag}} = \frac{qB_0}{m\,r^3}\left[-\left(\dot{\theta} - \omega_{\mathrm{e}}\right)\left(\sin^2\phi\,\hat{\boldsymbol{r}} + \sin 2\phi\hat{\boldsymbol{\phi}}\right) + \left(\frac{\dot{r}}{r}\sin\phi - 2\dot{\phi}\cos\phi\right)\hat{\boldsymbol{\theta}}\right]\,. \tag{11}$$

In the case of Lagrange's planetary equations, we need the perturbing force $\boldsymbol{F}_{\mathrm{mag}}$ to be decomposed into the radial, transverse and normal directions. The unit vector $\hat{\boldsymbol{n}}$ normal to the orbit is aligned with the angular momentum unit vector $\hat{\boldsymbol{h}}$, and the transverse unit vector $\hat{\boldsymbol{t}}$ can be calculated from the right-hand rule, $\hat{\boldsymbol{t}} = \hat{\boldsymbol{n}} \times \hat{\boldsymbol{r}}$,

$$\hat{\boldsymbol{n}} = \hat{\boldsymbol{h}} = (\boldsymbol{r} \times \boldsymbol{V})\,/\,\sqrt[2]{\mu p} = r^2/\sqrt{\mu p}\left(-\dot{\theta}\sin\phi\hat{\boldsymbol{\phi}} + \dot{\phi}\hat{\boldsymbol{\theta}}\right)\,, \tag{12}$$

where μ is the Earth's gravitational parameter and $p = a(1-e^2)$. Here, a and e are the semimajor axis of the orbit and the eccentricity of the satellite's orbit respectively.

Decomposition of the Lorentz force experienced by the geomagnetic field in the radial, transverse, and normal components yields (R_{mag}, T_{mag}, N_{mag}) respectively.

$$\begin{aligned} R_{\text{mag}} &= \boldsymbol{F}_{\text{mag}} \cdot \hat{\boldsymbol{r}} = \frac{q}{m}\frac{B_0}{r^3}\left[-r\dot{\theta}\sin^2\phi + \omega_{\text{e}}\sin^2\phi\right] , &(13)\\ T_{\text{mag}} &= \boldsymbol{F}_{\text{mag}} \cdot \hat{\boldsymbol{t}} = \frac{q}{m}\frac{B_0}{r^3}\left[2r\dot{\theta}\sin\phi\cos\phi - 2\omega_{\text{e}} r\cos\phi\sin\phi\right] , &(14)\\ N_{\text{mag}} &= \boldsymbol{F}_{\text{mag}} \cdot \hat{\boldsymbol{n}} = \frac{q}{m}\frac{B_0}{r^3}\left[\dot{r}\sin\phi - 2r\,\dot{\phi}\cos\phi\right] . &(15)\end{aligned}$$

The relationship between the spherical coordinates and the orbital elements is required to complete the derivation of Lagrange's planetary equations.

$$\begin{aligned} r &= a\left(1-e^2\right)/\left(1+e\cos f\right) , &(16)\\ \dot{r} &= e\sqrt{\mu/a\left(1-e^2\right)}\,\sin f , &(17)\\ \cos\phi &= \sin i\sin\left(\omega+f\right) , &(18)\\ \sin\phi &= \sqrt{1-\sin^2 i\sin^2\left(\omega+f\right)} , &(19)\\ \dot{\phi} &= \sqrt{\mu/a^3\left(1-e^2\right)^3}\frac{\sin i\cos\left(\omega+f\right)}{\sqrt{1-\sin^2 i\cos^2\left(\omega+f\right)}}\left(1+e\,\cos f\right)^2 , &(20)\end{aligned}$$

$$\dot{\theta} = \sqrt{\mu/a^3\left(1-e^2\right)^3}\frac{\cos i}{1-\sin^2 i\sin^2\left(\omega+f\right)}\left(1+e\,\cos f\right)^2 . \quad (21)$$

Here i, ω and f are the inclination of the orbit with respect to the equator, the argument of the perigee, and the true anomaly of the spacecraft orbit, respectively.

Therefore, rewriting the components of the Lorentz force due to the geomagnetic field as a function of the orbital elements, we obtain

$$\begin{aligned} R_{\text{mag}} &= \frac{q}{m}\frac{B_0}{r^3}\Bigg\{-\sqrt{\mu/a(1-e^2)}\cos i(1+e\cos f)\sin^2\phi \\ &\quad +\omega_{\text{e}}\Big[1-\sin^2 i\sin^2(\omega+f)\Big]\Bigg\} , &(22)\\ T_{\text{mag}} &= \frac{q}{m}\frac{B_0}{r^3}\sqrt{1-\sin^2 i\sin^2(\omega+f)}\sin i\sin(\omega+f) \\ &\quad \times\left[2\sqrt{\mu/a(1-e^2)}\frac{\cos i}{1-\sin^2 i\sin^2(\omega+f)}(1+e\cos f) - 2\omega_{\text{e}}\frac{a(1-e^2)}{(1+e\cos f)}\right] , &(23)\\ N_{\text{mag}} &= \frac{q}{m}\frac{B_0}{r^3}\left[\frac{\sqrt{\mu/a(1-e^2)}}{\sin f}\sqrt{1-\sin^2 i\sin^2(\omega+f)}\right. \\ &\quad \left. -\sqrt{\mu/a(1-e^2)}\frac{\sin^2 i\cos(\omega+f)\sin(\omega+f)}{\sqrt{1-\sin^2 i\cos^2(\omega+f)}}(1+e\cos f)\right] . &(24)\end{aligned}$$

Now we develop the Lorentz force due to the electric field $\boldsymbol{F}_{\text{elec}}$.

According to Ulaby (2005) and Heilmann et al. (2012) we can write the electric force as the following:

$$\boldsymbol{F}_{\text{elec}} = -\boldsymbol{\nabla} V_{\text{elec}} = \left(\frac{\partial V_{\text{elec}}}{\partial r}\hat{\boldsymbol{r}} + \frac{1}{r}\frac{\partial V_{\text{elec}}}{\partial\phi}\hat{\boldsymbol{\phi}} + \frac{1}{r\sin\theta}\frac{\partial V_{\text{elec}}}{\partial\theta}\hat{\boldsymbol{\theta}}\right) , \quad (25)$$

where $V_{\rm elec}$ is the electric potential,

$$V_{\rm elec} = \frac{\boldsymbol{P}\cdot\hat{\boldsymbol{r}}}{4\pi\epsilon_0 r^2}\,. \tag{26}$$

$\boldsymbol{P} = q\boldsymbol{d}$ is called the electric dipole moment, $\boldsymbol{d}$ is the distance vector from charge $-q$ to charge $+q$ and $\epsilon_0 = 8.85\times10^{-12}$ C$^2/(N-m^2) \equiv$ V^{-1} m^{-1} is the permittivity of free space.

Then the final form of the the Lorentz force experienced by an electric dipole moment in the presence of an electric field is

$$\boldsymbol{F}_{\rm elec} = \frac{qd}{4\pi\ \epsilon_0 r^3}\left(2\cos\phi\ \hat{\boldsymbol{r}} + \sin\phi\hat{\boldsymbol{\phi}} + 0\hat{\boldsymbol{\theta}}\right). \tag{27}$$

Similarly as we did for the magnetic force, we can write the radial, transverse and normal components ($R_{\rm elec}$, $T_{\rm elec}$, $N_{\rm elec}$) of the electric force,

$$\begin{aligned}
R_{\rm elec} &= \boldsymbol{F}_{\rm elec}\cdot\hat{\boldsymbol{r}} = -\frac{q}{m}\frac{d}{4\pi\ \epsilon_0 r^3}\left(\omega_{\rm e}-\dot{\theta}\right)\sin^2\phi\,, && (28)\\
T_{\rm elec} &= \boldsymbol{F}_{\rm elec}\cdot\hat{\boldsymbol{t}} = \frac{q}{m}\frac{d}{4\pi\ \epsilon_0 r^3}\frac{r^3}{\sqrt{\mu\ a\,(1-e^2)}}\left(\omega_{\rm e}-\dot{\theta}\right)\ \dot{\phi}\ \sin\phi\ \cos\phi\,, && (29)\\
N_{\rm elec} &= \boldsymbol{F}_{\rm elec}\cdot\dot{\boldsymbol{n}} = \frac{q}{m}\frac{d}{4\pi\epsilon_0 r^3}\frac{r^2}{\sqrt{\mu a\,(1-e^2)}}\left(\omega_{\rm e}-\dot{\theta}\right)\dot{\theta}\sin^2\phi\ \cos\phi\,. && (30)
\end{aligned}$$

Similarly, we can rewrite the components of the Lorentz force due to an electric field as a function of orbital elements as follows:

$$\begin{aligned}
R_{\rm elec} &= -\frac{q}{m}\frac{d}{4\pi\epsilon_0 r^3}\left[\omega_{\rm e}(1-\sin^2 i\sin^2(\omega+f)) - \sqrt{\mu/a^3(1-e^2)^3}\cos i(1+e\cos f)^2\right], && (31)\\
T_{\rm elec} &= \frac{q}{m}\frac{d}{4\pi\epsilon_0 r^2}\left[\omega_{\rm e} - \sqrt{\mu/a^3\,(1-e^2)^3}\frac{\cos i}{1-\sin^2 i\sin^2(\omega+f)}\,(1+e\ \cos f)^2\right]\\
&\quad\times\sin^2 i\cos(\omega+f)\sin(\omega+f)\ , && (32)\\
N_{\rm elec} &= \frac{q}{m}\frac{d}{4\pi\epsilon_0 r^3}\left[\omega_{\rm e} - \sqrt{\mu/a^3\,(1-e^2)^3}\frac{\cos i}{1-\sin^2 i\sin^2(\omega+f)}\,(1+e\cos f)^2\right]\\
&\quad\times\sin i\ \cos i\sin(\omega+f)\,. && (33)
\end{aligned}$$

3 LAGRANGE PLANETARY EQUATIONS WITH ACCELERATION FROM THE LORENTZ FORCE

It is logical to employ Lagrange's planetary equations in Gauss form to analyze the time rates of classical orbital elements resulting in acceleration from the total Lorentz force:

$$\frac{da}{dt} = \frac{2}{n\sqrt{1-e^2}}\Big[\,(R_{\rm mag}+R_{\rm elec})\,e\sin f + (T_{\rm mag}+T_{\rm elec})\,(1+e\cos f)\,\Big]\,, \tag{34}$$

$$\frac{de}{dt} = \frac{\sqrt{1-e^2}}{n\,a}\left[(R_{\mathrm{mag}}+R_{\mathrm{elec}})\sin f + (T_{\mathrm{mag}}+T_{\mathrm{elec}})\left(\frac{e\ +\cos f}{1+e\cos f}+\cos f\right)\right], \quad (35)$$

$$\frac{di}{dt} = \frac{r\ \cos(\omega+f)}{n\,a^2\sqrt{1-e^2}}\,(N_{\mathrm{mag}}+N_{\mathrm{elec}})\ , \quad (36)$$

$$\frac{d\Omega}{dt} = \frac{r\ \sin(\omega+f)}{n\,a^2\sqrt{1-e^2}\sin i}\,(N_{\mathrm{mag}}+N_{\mathrm{elec}})\ , \quad (37)$$

$$\begin{aligned}\frac{d\omega}{dt} &= \frac{\sqrt{1-e^2}}{n\,a\,e}\left[-(R_{\mathrm{mag}}+R_{\mathrm{elec}})\cos f + (T_{\mathrm{mag}}+T_{\mathrm{elec}})\left(1+\frac{r}{a\,(1-e^2)}\right)\sin f\right]\\ &\quad -\cos i\frac{d\Omega}{dt}\,, \quad (38)\end{aligned}$$

$$\begin{aligned}\frac{dM}{dt} &= \frac{1-e^2}{n\,a\,e}\Big[-(R_{\mathrm{mag}}+R_{\mathrm{elec}})\left(\cos f - 2e\frac{r}{a\,(1-e^2)}\right)\\ &\quad +(T_{\mathrm{mag}}+T_{\mathrm{elec}})\left(1+\frac{r}{a\,(1-e^2)}\right)\sin f\Big] - \cos i\frac{d\Omega}{dt}\,. \quad (39)\end{aligned}$$

4 NUMERICAL RESULTS

In this section, we consider the numerical simulation for verification of the derived perturbations in the orbital motion of a spacecraft due to the Lorentz force, using Lagrange's planetary Equations (34)–(38). We can apply those equations to get the perturbation in the orbital elements due to the total Lorentz force or due to the separate magnetic and electric components of the Lorentz force. From Equations (22)–(23) and Equations (31)–(33), we note that the components of the Lorentz force due to the magnetic and electric fields are proportional to the charge to mass ratio. This means that with this ratio we can control the orbital motion of a satellite.

Figure 2 displays the variation in the semimajor axis due to the magnetic component of the Lorentz force at different values for inclination and argument of perigee with a charge of 100 C. The perturbation could reach 40 km depending on the amount of charge and the type of orbit. We notice that the peak in perturbation occurs for polar orbits when the inclination is close to 90° and the argument of perigee is around 0°, 180° and 360°.

Figure 3 explains the variation in the semimajor axis due to the electric component of the Lorentz force at different values for inclination and argument of perigee with a charge of 100 C. The perturbation could reach 100 km depending on the charge and the type of orbit. Similarly, the peak of perturbation occurs at the polar orbits when inclination is close to 90° and the argument of perigee is around 0°, 180° and 360°.

Figure 4 shows the variation in the semimajor axis due to the magnetic component of the Lorentz force with different charges and arguments of perigee, and an inclination of $i = 52°$. The peak in perturbation is 10 km and depends on the value of charge and when the argument of perigee is around 0°, 180° and 360°.

Figure 5 shows the variation in semimajor axis due to the electric component of the Lorentz force with different charges and arguments of perigee, and an inclination of $i = 52°$. The peak in the perturbation is 4 km and depends on the value of charge and when the argument of perigee is around 0°, 180° and 360°.

Figures 6–9 show the time variation of the semimajor axis, eccentricity, inclination, argument of perigee and the longitude of the ascending node for an LEO after two days, respectively (where the perturbation only involves the Lorentz force). Each figure presents two different cases, i.e. the perturbation due to the magnetic component of the Lorentz force represented by a solid line, and the dotted line representing the perturbation due to the electric component. We have used the ratio $q/m = 0.0393$ C kg^{-1} in Equations (34)–(38).

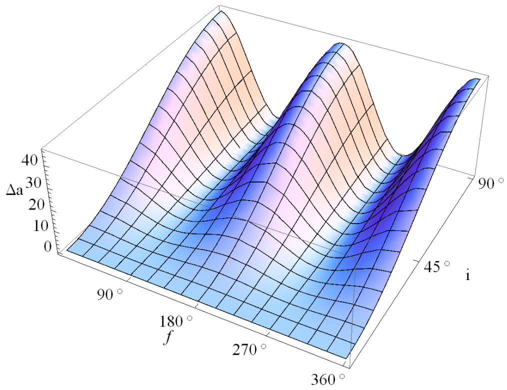

Fig. 2 The variation in the semimajor axis due to the magnetic component of the Lorentz force with different values of inclination and true anomaly, with $q = 100\,\mathrm{C}$ and $m = 300\,\mathrm{kg}$.

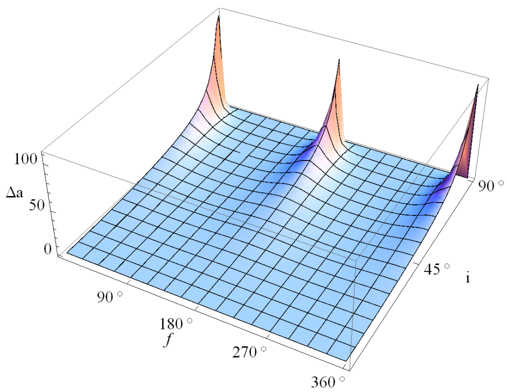

Fig. 3 The variation in the semimajor axis due to the electric component of the Lorentz force with different values of inclination and true anomaly, with $q = 100\,\mathrm{C}$ and $m = 300\,\mathrm{kg}$.

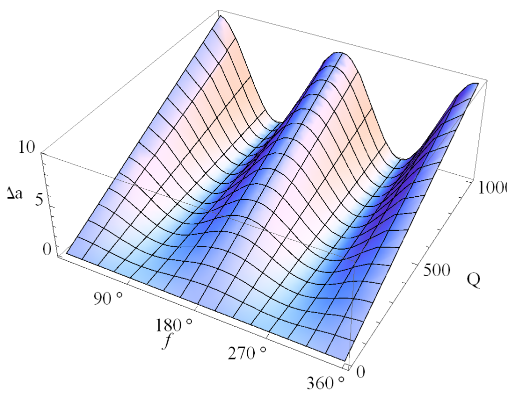

Fig. 4 The variation in the semimajor axis due to the magnetic component of the Lorentz force with different values of charge and true anomaly, with $i = 52^\circ$ and $m = 300\,\mathrm{kg}$.

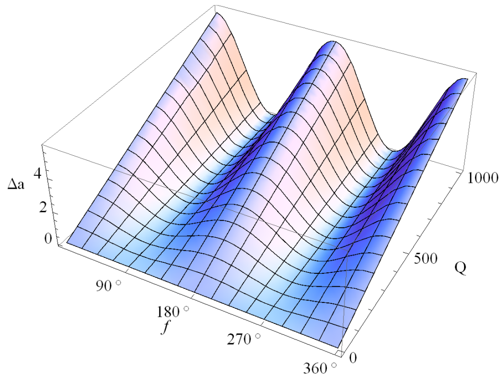

Fig. 5 The variation in the semimajor axis due to the electric component of the Lorentz force with different values of charge and true anomaly, with $i = 52°$ and $m = 300\,\mathrm{kg}$.

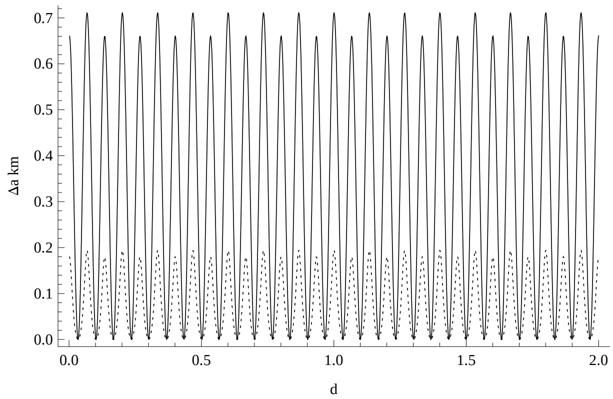

Fig. 6 Time rate of change in the semimajor axis for an LEO with $q/m = 0.0393$ C kg^{-1}, $a = 6900\,\mathrm{km}$, $e = 0.005$, $i = 52°$, $m = 297\,\mathrm{kg}$, $q = 117\,\mathrm{C}$, $\omega = 293°$ and $f = 293°$.

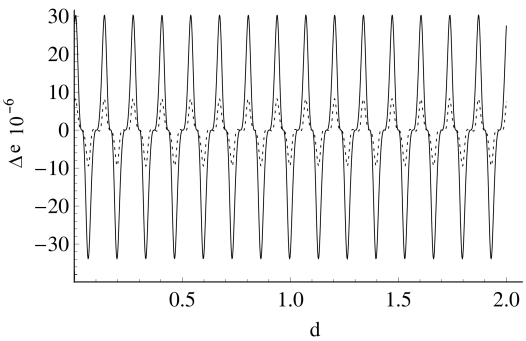

Fig. 7 Time rate of change in the eccentricity for an LEO, with $q/m = 0.0393$ C kg^{-1}, $a = 6900\,\mathrm{km}$, $e = 0.005$, $i = 52°$, $m = 297\,\mathrm{kg}$, $q = 117\,\mathrm{C}$, $\omega = 293°$ and $f = 293°$.

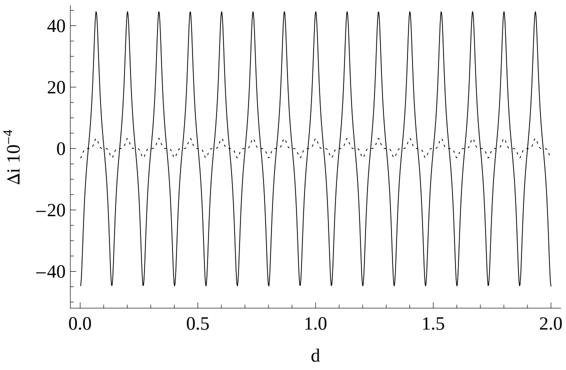

Fig. 8 Time rate of change in the inclination for an LEO, with $q/m = 0.0393\,\mathrm{C\,kg^{-1}}$, $a = 6900\,\mathrm{km}$, $e = 0.005$, $i = 52°$, $m = 297\,\mathrm{kg}$, $q = 117\,\mathrm{C}$, $\omega = 293°$ and $f = 293°$.

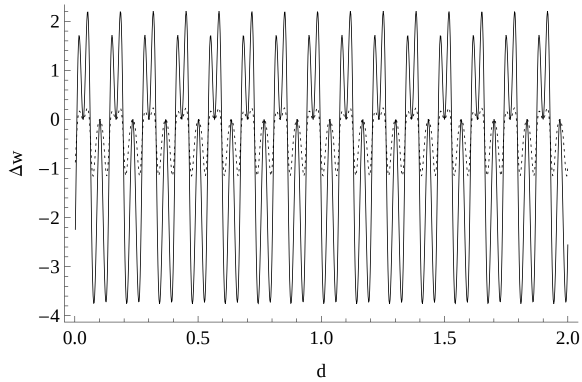

Fig. 9 Time rate of change in the argument of perigee for an LEO, with $q/m = 0.0393$ C kg^{-1}, $a = 6900\,\mathrm{km}$, $e = 0.005$, $i = 52°$, $m = 297\,\mathrm{kg}$, $q = 117\,\mathrm{C}$, $\omega = 293°$ and $f = 293°$.

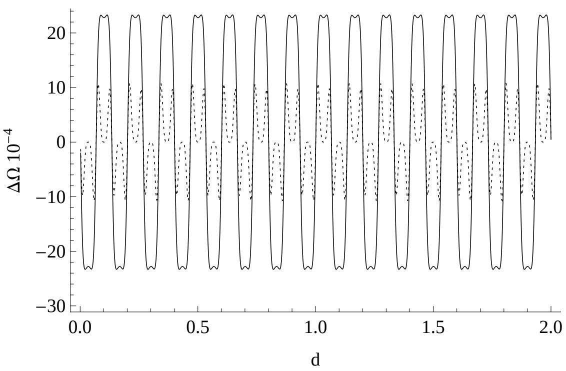

Fig. 10 Time rate of change in the ascending node for an LEO, with $q/m = 0.0393$ C kg^{-1}, $a = 6900\,\mathrm{km}$, $e = 0.005$, $i = 52°$, $m = 297\,\mathrm{kg}$, $q = 117\,\mathrm{C}$, $\omega = 293°$ and $f = 293°$.

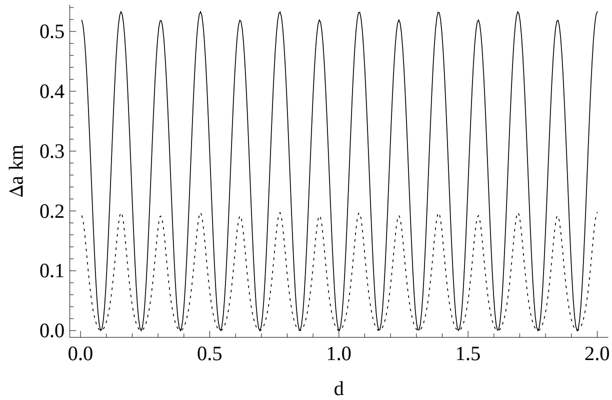

Fig. 11 Time rate of change in the semimajor axis for a Lageos satellite, with $q/m = 0.0393$ C kg^{-1}, $a = 12\,300$ km, $e = 0.0001$, $i = 53°$, $m = 407$ kg, $q = 160$ C, $\omega = 187°$ and $f = 225°$.

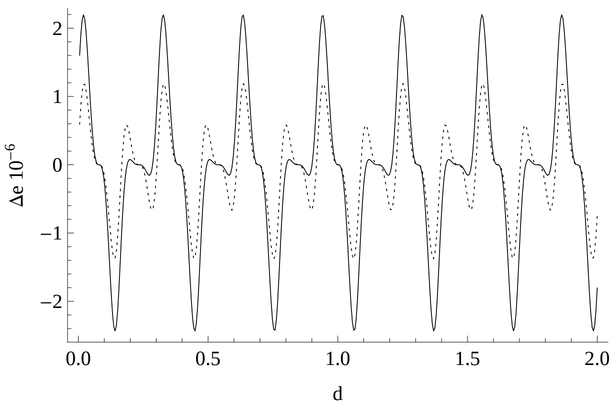

Fig. 12 Time rate of change in the eccentricity for a Lageos satellite, with $q/m = 0.0393$ C kg^{-1}, $a = 12\,300$ km, $e = 0.0001$, $i = 53°$, $m = 407$ kg, $q = 160$ C, $\omega = 187°$ and $f = 225°$.

The figures show that the perturbation in the orbital elements is periodic and is a second order perturbation. The perturbations in the semimajor axis are about 0.7 km after two days due to the magnetic force and about 0.2 km due to the electric force. This means that the electric component of the Lorentz force is still an important element to take into account.

Figures 11–15 show the time variation in the orbital elements of the Lageos satellite with the same ratio of $q/m = 0.0393$ C kg^{-1}. Similarly, the figures show that the perturbation in the orbital elements is periodic and is a second order perturbation. The perturbation in the semimajor axis is about 0.5 km after two days due to the magnetic force and is about 0.2 km due to the electric force. Comparing the results for an LEO satellite and a Lageos satellite, we note that an Lorentz force is more effective when applied to the LEO. We conclude that the Lorentz force, with a sufficient amount of charge, could be used to compensate for the orbital drift resulting from perturbations in formation of satellites, particulary for an LEO.

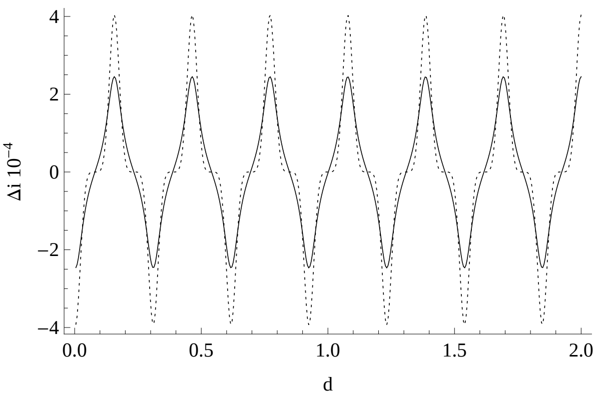

Fig. 13 Time rate of change in the inclination for a Lageos satellite, with $q/m = 0.0393$ C kg^{-1}, $a = 12\,300$ km, $e = 0.0001$, $i = 53°$, $m = 407$ kg, $q = 160$ C, $\omega = 187°$ and $f = 225°$.

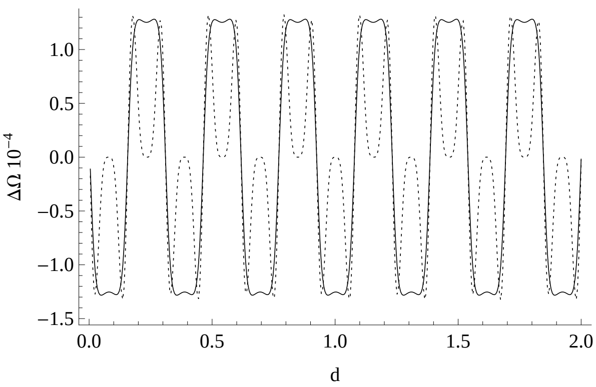

Fig. 14 Time rate of change in the ascending node for a Lageos satellite, with $q/m = 0.0393$ C kg^{-1}, $a = 12\,300$ km, $e = 0.0001$, $i = 53°$, $m = 407$ kg, $q = 160$ C, $\omega = 187°$ and $f = 225°$.

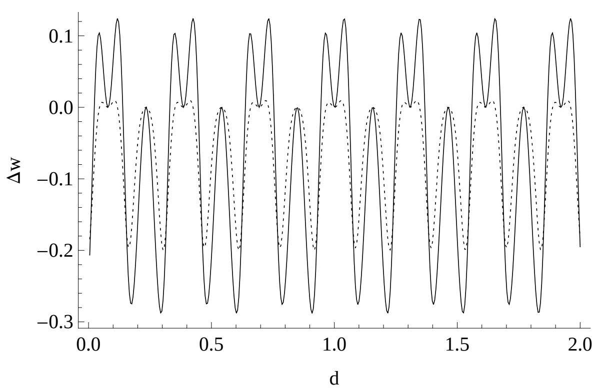

Fig. 15 Time rate of change in the argument of perigee for a Lageos satellite, with $q/m = 0.0393$ C kg^{-1}, $a = 12\,300$ km, $e = 0.0001$, $i = 53°$, $m = 407$ kg, $q = 160$ C, $\omega = 187°$ and $f = 225°$.

5 CONCLUSIONS

The Lorentz force is developed in two cases: (1) Lorentz force that results from the geomagnetic field and (2) Lorentz force experienced by an electric dipole moment in the presence of an electric field. The Lorentz force is derived as a function of orbital elements. Gauss variational equations are admitted for time rate of change in the orbital elements of a spacecraft. The Lorentz force is developed on the basis of charge to mass ratio as a factor that can control effects from the Lorentz force. The numerical results have shown the strong effects of the Lorentz force on the orbital motion of a spacecraft. The perturbation in the orbital elements is a second order perturbation. The numerical results confirm that the effect of the Lorentz force due to the geomagnetic field is about three times that of the Lorentz force experienced by the electric field. The results demonstrate that the effects of the Lorentz force increase in highly inclined orbits which are close to a polar orbit. As shown in Figure 4, we conclude that the Lorentz force has strong perturbations in the semimajor axis that depend on the amount of charge. The values of charge and mass of a satellite are key for controlling the effects of the Lorentz force. For example, when the value of charge is 117 C, and the mass of the satellite is 297 kg (see Fig. 6), the perturbation in the semimajor axis is 0.7 km after three days. When the value of charge is 160 C and the mass of the satellite is 407 kg (see Fig. 11), the perturbation in the semimajor axis is 0.5 km after three days. Therefore, we can simply insert a device onboard the spacecraft to artificially generate the desired amount of charge in order to control the orbital motion of the spacecraft or to compensate for other perturbations.

References

Abdel-Aziz, Y. A. 2007, AMS, 1, 1511 (*http://www.m-hikari.com/ams/ams-password-2007/ams-password29-32-2007/abdelazizAMS29-32-2007.pdf*)

Ciufolini, I., Farinella, P., Nobili, A. M., Lucchesi, D., & Anselmo, L. 1993, Nuovo Cimento B Serie, 108, 151

Heilmann, A., Ferreira, L. D. D., & Dartora, C. A. 2012, Brazilian Journal of Physics, 42, 55

Juhász, A., & Horányi, M. 1997, J. Geophys. Res., 102, 7237

Peck, M. A. 2005, in AIAA Guidance, Navigation and Control Conference (San Francisco: CA, AIAA) 2005–5995

Pollock, G. E., Gangestad, J. W., & Longuski, J. M. 2011, Acta Astronautica, 68, 204

Sehnal, L. 1969, SAO Special Report, 271

Streetman, B., & Peck, M. A. 2007, Journal of Guidance Control Dynamics, 30, 1677

Ulaby, F. T. 2005, Electromagnetics for Engineers (Pearson/Prentice Hall)

Vokrouhlicky, D. 1989, Celestial Mechanics and Dynamical Astronomy, 46, 85